Article

pubs.acs.org/Biomac

Binding of Starch Fragments to the Starch Branching Enzyme: Implications for Developing Slower-Digesting Starch

Rob Marc Go,[†,‡] Alan E. Mark,[§,⊥] Alpeshkumar K. Malde,[*,§] and Robert G. Gilbert[*,†,‡]

[†]Tongji School of Pharmacy, Huazhong University of Science and Technology, Wuhan, China, 430030

[‡]Centre for Nutrition and Food Science, Queensland Alliance for Agriculture and Food Innovation, [§]School of Chemistry and Molecular Biosciences, and [⊥]Institute for Molecular Biosciences, The University of Queensland, Brisbane, Queensland 4072, Australia

Supporting Information

ABSTRACT: Molecular weight distributions of starch branches affect functional properties, which can be controlled by engineering starch branching enzymes (SBEs). Molecular dynamics and docking approaches are used to examine interactions between SBE and starch fragments. In the native protein, three residues formed stable interactions with starch fragments in the central binding region; these residues may play key roles in substrate recognition. Fragments containing 5−12 glucose units interacted more tightly with SBE than smaller fragments, suggesting a minimal functional fragment size of 5, agreeing with experiment. Effects of three different point mutations on interactions with maltopentaose in the central binding region correlated well with experiment. Simulations indicate that SBE may template formation of the crystalline lamellae characteristic of native starch, consistent with the observation that crystalline lamellae formed by starch in a plant, are not necessarily the state of lowest free energy. The methodology will help develop starches with optimized functional properties.

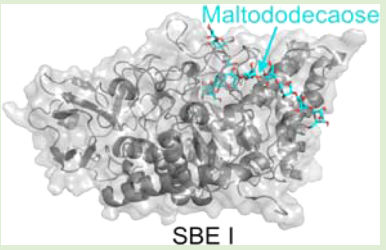

INTRODUCTION

Starch is a highly branched glucose polymer and the most important dietary carbohydrate. It is found in two main forms, which differ in terms of the nature of their branching: amylose is a primarily linear polymer containing a few long branches, while amylopectin is a highly branched structure containing a large number of short branches. Both have α-(1 → 4) glycosidic bonds forming the linear chains and branch points formed via α-(1 → 6) glycosidic bonds.

Many functional properties of starch-containing substances are influenced by the chain (branch) length distribution: the CLD. Two of the most important properties are the rate and location of the digestion of starch-based foods. The consumption of slower digesting starches and resistant starches is considered beneficial, aiding in both the prevention and management of diet-related illnesses such as type-II diabetes, obesity and colo-rectal cancer.[1,2] For example, Zhang et al.[2] reported that starch with a degree of polymerization (DP) of 13 was most rapidly digested and that amylopectin molecules containing either a higher proportion of short branches or a higher proportion of longer branches were digested more slowly.[2] The longer amylopectin chains (DP > 13) are believed to be enzyme-resistant due to the formation of linear helices.[3] Changes in the CLD can result from variations (point mutations) in a range of starch biosynthetic enzymes, producing different starch products.

Starch is synthesized in a multistep process through the concerted action of several enzymes. The addition of glucose units to an existing chain is performed by starch synthase (SS), the production of branched chains by starch branching enzyme (SBE) and the debranching of branched structures by starch debranching enzyme (DBE). SBE is the sole enzyme that introduces branches to the linear starch chain.[4] It creates α-(1 → 6) glycosidic bonds by internally cleaving an α-(1 → 4) glycosidic bond and reintroducing it to a free C6 hydroxyl group.[5] SBE exists in multiple isoforms, with the number and types of isoforms present being dependent on the plant species.[6] In rice (*Oryza sativa L.*), there are three notable isoforms: SBEIa, SBEIIa, and SBEIIb. SBEI has been associated with the transfer of longer chains, and is thought to have a greater effect on amylose synthesis, while SBEII transfers shorter chains and increases the number of branches of amylopectin.[7] In rice, it has been determined that SBEIa and SBEIIb preferably transfer chain lengths of DP ∼10 and 3−9, respectively.[7]

SBE belongs to the α-amylase family and is categorized as a transferase, which can cleave either α-(1 → 4) or α-(1 → 6) glycosidic bonds. As illustrated in Figure 1, α-amylases have a TIM-barrel structure with the catalytic site lying within the central cleft of the $(\beta/\alpha)_8$-barrel (this and later figures were made using PyMOL v1.6.x[8]). The region in red in this figure represents the part of the N-terminal region where the maltopentaose binds in the structure 3VU2.[9] Residues in the central binding region identified by Vu at al. to be catalytically important, namely Tyr235, Asp270, His275, Arg243, Asp344, Glu399, and His467, are shown in the inset in green.[10] Vu et al.

Received: May 25, 2015
Revised: June 25, 2015
Published: June 26, 2015

DOI: 10.1021/acs.biomac.5b00710
Biomacromolecules 2015, 16, 2475−2481

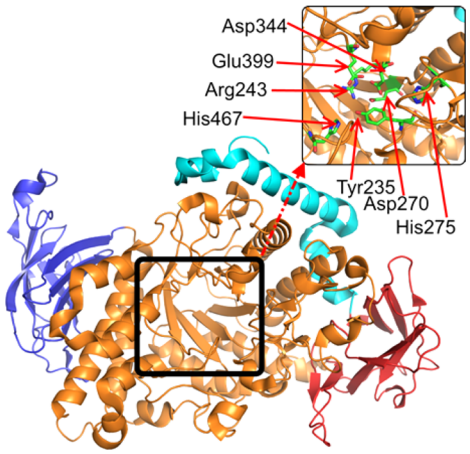

Figure 1. A ribbon representation of the SBEI structure 3AML showing the conserved α-amylase domains; the N-terminal region (cyan + red), the central β/α_8-barrel (orange), and the C-terminal domain (blue). See text for other details.

also reported that Glu399 and Asp344 act as an acid/base catalyst and as a nucleophile, respectively, and His275 and His467 may aid in the distortion and stabilization of the starch fragment, respectively.[10] These amylases hydrolyze α-glycosidic bonds, producing α-anomeric, mono- or oligosaccharides forming either or both α-(1 → 4), α-(1 → 6) glycosidic bonds.[11] Not only do α-amylases share common structural characteristics but they also contain several highly conserved amino acids. These include a glutamic acid that acts as an acid/base catalyst, an aspartic acid which acts as a nucleophile, and a group of histidine, arginine and tyrosine residues that aid the stabilization and orienting of the substrate.[11,12]

For transfer by SBE to occur, two size requirements must be meet: the DP of the chain to be moved must be greater than or equal to a minimum value, denoted $X_{min,}$ and the DP of the remaining fragment must be greater than or equal to a minimal value denoted X_0.[13] An analysis of fragmentation data suggests values $X_0 \sim 6$ and $X_{min} \sim 10$. For example, in mSBEIIa (*Zea mays*) it has been found that the minimum chain length for either X_{min} or X_0 is 6.[14] Similar results were found in *Arabidopsis*.[13,15]

Currently, three crystal structures of rice SBE (derived from *Oryza sativa L.*) are available in the protein data bank (3AML, 3VU2 and 3AMK). 3AML and 3AMK were solved at a resolution of 1.70 and 1.90 Å respectively, and represent the apo forms of the enzyme.[16] 3AMK is the mature native enzyme and contains 755 residues, while the 3AML structure contains 702 residues. Notably, 3AML exhibits some electron density in the central region. While the origin of this density is unknown, it has been proposed that this corresponds to a small amount of residual substrate and thus reveals a potential sugar binding site. 3VU2, solved at a resolution of 2.23 Å, was cocrystallized with maltopentaose and two glucose moieties. The maltopentaose was found to bind to a part of the N-terminal region (shown in red in Figure 1).[9] The individual glucose molecules were also loosely associated with the N-terminal region. 3VU2 has a single point mutation at the catalytically important Glu399 (E399Q). However, Chaen et al.[9] reported that this mutation did not change the central binding site. Based on their structure, they proposed that the substrate bound initially to the N-terminal region, possibly causing a conformational change within the central cleft that allowed for further binding and the enzymatic reaction.

Experiments by Li et al.[14] introduced five different single-point mutations (Y235F, E399D, S232F, R342K and R246K; numbering as in SBEI) into SBEIIa derived from corn (*Zea mays*). These residues were chosen because they are highly conserved in a variety of α-amylase enzymes. In addition, Tyr235, Glu399, and Arg342 residues lay within the vicinity of a region of "unknown electron density" observed in the crystal structure of 3AML. Li et al.[14] found that mutations in the central binding region including Y235F, E399D, and S232F led to an overall loss of branching activity. R342K led to a slight decrease in activity and a higher amount of shorter branches (DP $\leq$ 3). By contrast, R246K, which lies on the opposite side of the enzyme facing away from the central binding region, led to no change in activity.

To rationalize these observations in terms of a structural model, a detailed understanding how these residues might interact with a potential substrate is required. Such understanding can lead to the rational choice of mutations needed to engineer an SBE that would, when inserted into a plant, give starch with desirable nutritional properties. Although the structure of no corn SBEs is known, rice (*Oryza sativa L.*) SBEI and corn (*Zea mays*) SBEIIa share 60% similarity and 49% sequence identity. In particular, the central cleft binding site is highly conserved. This suggests that lessons learned from the studies on corn could in principle be transferred to the rice, especially as, with the exception of S232F, the mutations examined by Li et al.[14] were structurally conservative. Here, a combination of molecular dynamics (MD) simulations and docking approaches have been used to examine the binding of a range of sugar oligomers of chain lengths 3, 4, 5, 6, 8, 10, and 12 (maltotriose, maltotetraose, maltopentaose, maltohexaose, maltooctaose, maltodecaose and maltododecaose) to rice SBE. The aim was to complement and help interpret the available experimental data in order to develop a better understanding of starch binding to SBEs more generally. In addition, the crystal structure 3VU2 was used to study the binding of maltopentaose to the N-terminal region of the protein. The effect of the mutation E399Q on the binding of different sugars is also examined. Finally, the effect of the mutations R342K, E399D, and Y235F on the binding of maltopentaose was examined again to rationalize experimental observations.

METHODS

Computational Details. All MD simulation and docking studies reported in this study were performed on structures 3AML and 3VU2 derived from the protein databank (PDB). 3AML was crystallized as a monomer, while 3VU2 was crystallized as a symmetric dimer. The only difference between the two structures was a glutamic acid (E399) in 3AML, which was mutated to glutamine (Q399) in 3VU2. All substrate-enzyme simulations used the 3AML crystal structure, while Chain-A of 3VU2 crystal structure was used to study the mutation E399Q and the stability of the N-terminal region binding site.

All MD simulations were performed using the GROMACS simulation program version 3.3.3.[17] The GROMOS54A7 force-field was used to describe interactions involving the protein.[18] The starch molecules were described using the optimized GROMOS sugar parameters developed as part of the GROMOS 45A4 force field.[19] The parameters of the seven sugar fragments used are available from the Automated

DOI: 10.1021/acs.biomac.5b00710
Biomacromolecules 2015, 16, 2475−2481

Topology Builder (ATB).[20] The docking of seven starch fragments containing 3, 4, 5, 6, 8, 10, and 12 α-(1 → 4)-glucose units were modeled into the protein.

Full details of the simulations are given in the Supporting Information (SI).

Mutations. Three mutations, E399D, Y235F, and R342K (SBEI numbering), were introduced into both the truncated 3AML structure and the truncated 3AML to which maltopentaose had been docked using the PyMOL mutagenesis tool. The structures were verified using the swiss-pdb viewer to ensure no bad contacts or overlaps were present.[8,21] These systems were then solvated and equilibrated as outlined above. Each system was then simulated twice for 25 ns with different starting velocities.

Analysis. To identify the predominate conformations sampled during the simulation, the trajectories were clustered using the method of Daura et al.,[22] as implemented in the GROMACS package version 3.3.3.[17] Specifically, the backbone root-mean-square positional deviation (RMSD) of residues within well-defined regions of secondary structure (α-helices and β-sheets) between all possible pairs of structures were determined. For each structure, the number of neighbors for which the RMSD was less than or equal to a specified value was then determined. The structure with the highest number of neighbors was taken as the center of the first cluster. This structure and all of its neighbors were then eliminated from the pool of structures and the process repeated to identify subsequent clusters. To select appropriate values for the RMSD, in each case the distribution of RMSD values were analyzed to ensure that a clear separation of different clusters was obtained. Plots showing the distribution of RMSD values for each system are provided as SI (Figures S2 and S4).

RESULTS AND DISCUSSION

The systems investigated included the full-length structure of SBEI containing the mutation E399Q and maltopentaose bound within the N-terminal region (3VU2[9]). A truncated version of SBEI (lacking the C-terminal region of 588−699) based on the crystal structure 3AML, which has "unknown electron density" in the central binding region, was used to understand the binding of different sugars to the native protein. For this purpose, starch fragments containing 3, 4, 5, 6, 8, 10, and 12 glucose units were docked into this density. A truncated version of SBEI was used in this aspect to improve computational efficiency; the C-terminal region is not involved in starch binding. The 3VU2 structure (E399Q) with maltopentaose docked into the central binding region was also examined. Finally, the truncated 3AML structure was used to examine the effect of the other three single-point mutations mentioned above.

Configuration of Pro195 in 3VU2. The structure 3VU2 contains rice SBEI cocrystallized with maltopentaose and two glucose moieties bound within the N-terminal region. Initial simulations of the structure revealed abnormally large forces in the region of Pro195 leading to local distortions and the failure of the bond constraint algorithm. In 3VU2, Pro195 is modeled in a trans-configuration in both chains. However, examination of the Fo−Fc electron density map clearly indicates a significant region of positive density in the vicinity of this residue. This suggests that the structure does not adequately represent the observed data and that atoms in this region are missing. Detailed figures showing this region of the structure are provided as SI (Figure S1). Flipping Pro195 from the trans configuration to the statistically more common cis configuration moves the proline ring toward the positive Fo-Fc density and results in a reorientation of the surrounding atoms. The resulting structure was found to be stable in two independent simulations, each 25 ns in length. Indeed, cluster analysis of the combined trajectories using a RMSD cutoff of 0.2 nm revealed a single predominate cluster. The presence of a cis-Pro could be further confirmed by the rerefinement of the crystal structure.

The Binding of Maltopentaose to the N-Terminal Region of 3VU2. Based on the 3VU2 structure, Chaen et al.[9] proposed that maltopentaose bound primarily to the N-terminal region, due to stacking interactions formed with Phe100 and Trp319. A range of polar residues including His44, Glu45, Lys99, His294, Glu295, Glu320, and Arg323 were also proposed to interact with different sugar rings.[9] However, in the simulations that do not have restrictions imposed by the crystal environment, only Glu320 and Trp319 maintained an interaction with the maltopentaose, suggesting that Glu320 and Trp319 are the primary residues associated with the binding of maltopentaose to the N-terminal region. This is illustrated in Figure 2, which shows a region from the central member of the predominate cluster superimposed onto the starting 3VU2 crystal structure. The interactions between specific residues and the maltopentaose were also examined by monitoring the minimum distance between the residue and the maltopentaose over the trajectory. In the case of Glu320 and Trp319, the interactions formed within the first 5 ns and remained constant for the duration of the simulation. By contrast, the other residues proposed by Chaen et al.[9] to bind to maltopentaose in the crystal structure did not form stable interactions. Sample plots for Glu320 and Glu45 are provided as SI (Figure S3).

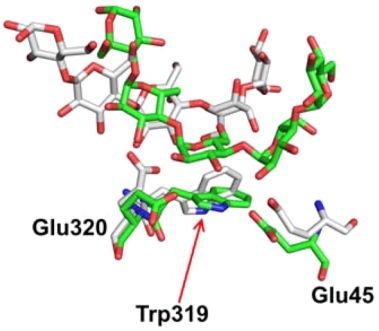

Figure 2. Stick representation of the maltopentaose from the crystal structure 3VU2 (green) superimposed onto that from the central member of the highest populated cluster from the combined 50 ns trajectory (gray). The positions of Glu320, Trp319, and Glu45 in the two structures are also indicated.

The question still remains as to whether this site is functionally important. Chaen et al.[9] proposed that the site could be the first site to which starch binds, leading to the opening of the central cleft. No change in the conformation of the central cleft was observed, however, during the 25 ns of simulation. While this could be due to the limited time simulated, the current study does not support the conformational change proposal.

Binding of Starch Fragments to Native SBE. To understand how starch molecules (or fragments) may bind to the native form of rice SBEI, a range of starch fragments

DOI: 10.1021/acs.biomac.5b00710
Biomacromolecules 2015, 16, 2475−2481

containing 3, 4, 5, 6, 8, 10, and 12 glucose units were docked into the central cleft of the 3AML structure, as described in the Methods. In each case, the systems were simulated in duplicate for 25 ns with different starting velocities. For those systems that contained starch polymers with DP ≥ 5, stable interactions were found to be formed with three residues Glu399, His467, and Trp309 in the majority of cases. In each case, the residues remained within a hydrogen-bonding distance. The shorter starch polymers (DP < 5) did not form stable interactions with these residues, with the distances varying between 0.8 and 1.6 nm. This is illustrated in Figure 3, which shows the minimum

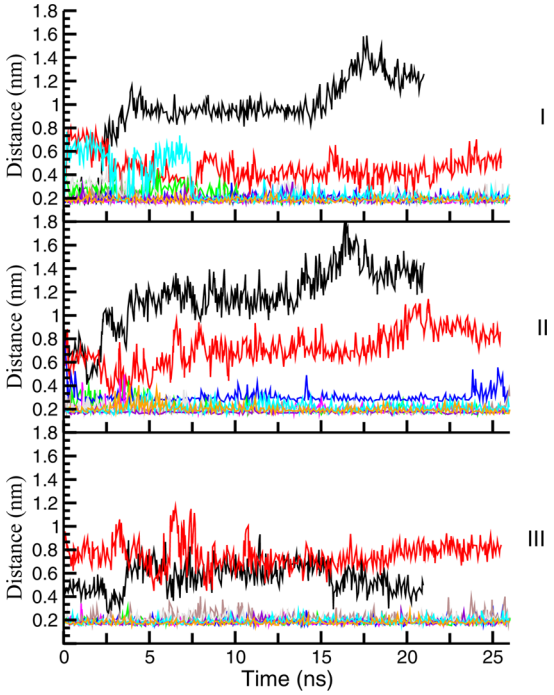

Figure 3. Minimum distance between any atom in the three different residues (I) Glu399, (II) His467, and (III) Trp309, with any atom of the different sized fragments (DP 3 (black), DP 4 (red), DP 5 (green), DP 6 (blue), DP 8 (magenta and violet (different positions)), DP 10 (brown and cyan (different positions)) and DP 12 (gray and orange (different positions)), over 25 ns. Similar results were obtained in the duplicate runs.

distance between any atom in one of these three residues and any atom in the different sized starch polymers over one of the 25 ns simulations. Similar results were obtained in duplicate runs.

The distances between Glu399-substrate, His467-substrate, and Trp309-substrate was measured over 25 ns. Maltotriose (black) and maltotetraose (red) did not form any stable interaction with Glu399 (Figure 3I), His467 (Figure 3II) or Trp309 (Figure 3III). The fact that neither maltotriose nor maltotetraose formed stable interactions with either Glu399 and His467, residues that are known to be catalytically important, may suggest that they have a lower affinity to bind to the central binding cleft than the longer substrates. Indeed it has been shown previously that the minimum DP corresponding to either X_{min} or X_0 in corn mSBEIIa and *Arabidopsis* is 6.[13−15] Given that, in the simulations, maltopentaose formed quite stable bonds with Glu399, His467, and Trp309 while maltotetraose did not, we predict that, in the case of rice SBEI, X_0 = 5. As noted above, Glu399 and His467 are known to be catalytically important. As far as we know, Trp309 has not been shown to be catalytically important. Tryptophans are, however, known to interact with oligosaccharides, and Trp309 could play a role in helping to bind the starch fragments.[23]

Helical Structure Bound in the Central Cleft. In the simulations of the enzyme:starch complexes, the sugar polymers were initially modeled in a random coil conformation. However, fragments with a DP ≥ 8 spontaneously adopted a helical-like structure within 10 ns. This is illustrated in Figure 4, which shows the initial conformation of maltododecaose in the central cleft of the SBE:maltodecaose system (Figure 4I) alongside the final structure from the simulations (Figure 4II). Additional details are provided as SI (Figures S5 and S6).

Starch has a complex hierarchical structure of which there are six identifiable levels.[24] The most basic of these levels relate to the nature and extent of branching. At a higher level, starch in a plant forms highly ordered units comprising helical structures in crystalline lamella.[24] The results obtained here would be compatible with the possibility that, after cleavage of the α-(1 → 4) glycosidic bond, the free chain could form a helical structure before being reattached to a free C6 hydroxyl group. To determine whether the helical conformation illustrated in Figure 4II is an intrinsic property of the starch fragment as described by the force field used, or is induced by the presence of the enzyme, simulations of a series of starch fragments (DP 8, 10, and 12) free in solution were performed to see if they adopt a helical-like structure on the same time scale as that observed in the substrate-enzyme simulations (10 ns).

In the case of maltooctaose, the fragment remained essentially linear within the 10 ns simulated. As the number of glucose units was increased to DP 10 and 12, the chain did begin to adopt a more coil-like conformation. However, in no case did these starch polymers form helical structures to the extent of that observed in the presence of enzyme. Seviour et al.[25] observed the formation of antiparallel double helices in sugar polymers corresponding to the repeating unit of granulation, using the same force field. Clearly, the length of the fragment plays a major role in determining its conformation in solution, with longer fragments favoring helical structures.[25] Interaction with SBE appears to promote the formation of helical-like structures in short fragments: the enzyme may thus act as a chaperone in the formation of crystalline lamellae in native starch. This inference is important in understanding the fact that while crystalline lamellae are formed in a plant, they are not the state of lowest free energy: when crystalline starch is annealed, or reformed after dissolution in a solvent, much of the crystalline structure disappears. Snapshots from the simulations of the isolated starch fragments in solution are provided as SI (Figure S7).

Effect of E399Q on the Binding of Maltopentaose to the Central Binding Cleft. 3VU2 contains the mutation E399Q in the central binding cleft. To understand whether this mutation is responsible for the binding of maltopentaose to the N-terminal region of SBEI, maltopentaose was docked into the central binding cleft of 3VU2 at the location of the unknown electron density as found in the crystal structure 3AML.[16] The resulting complex was simulated for 2 × 25 ns. This lead to an optimization of the complex and demonstrated that it was at least metastable in free solution. Cluster analysis of the combined 50 ns trajectory using a cutoff of 0.16 nm (see SI Figure S4) (E399Q)) revealed two major clusters. Figure 5I shows the interactions between the starch fragment and residues in the central cleft in the central member of the

DOI: 10.1021/acs.biomac.5b00710
Biomacromolecules 2015, 16, 2475−2481

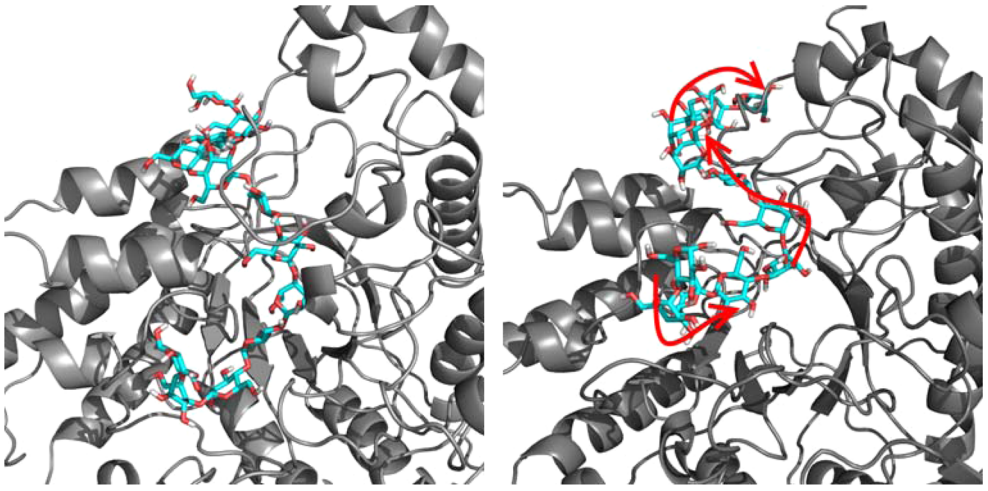

Figure 4. (I) Initial conformation of maltododecaose in the central binding cleft. (II) Final conformation after 25 ns of simulation. Similar results were obtained in the duplicate run. The arrows trace the curvature of the fragment.

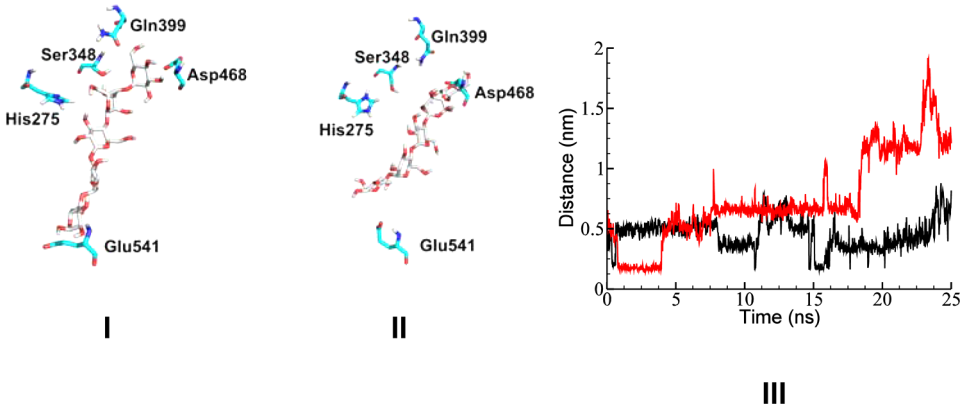

Figure 5. Central members of the two dominate clusters, I and II, from 2 × 25 ns simulations of 3VU2 with maltopentaose bound in the central cleft, showing the starch molecule and surrounding residues. (III) Plot of the minimum distance between the side chain amide O of Gln399 and the closest atom of maltopentaose in the two 25 ns trajectories.

largest cluster, which contained ~50% of the structures. In this structure, Ser348, Asp468, His275, and Glu541 interact directly with the maltopentaose. Figure 5II shows the equivalent interactions in the second most populated cluster, which contained 43% of the total structures. Glu399 is known to be functionally important and acts as an acid/base catalyst during the cleavage of the starch chain.[10] As expected, Glu399 forms quite stable interactions with maltopentaose in the simulations of the native protein (Figure 3I). In the 3VU2:maltopentaose system, the interactions between Gln399 and the maltopentaose are much more transient in nature. This is illustrated in Figure 5III, which shows the distance between the side chain O atom of Gln399 and the closest atom of maltopentaose (the hydrogen or hydroxyl group attached to carbon 6 of ring 5) during the two 25 ns trajectories. As can be seen in one trajectory, the distance varies between 0.2 and 0.6 nm, while in the other, the distance reaches more than 1.2 nm after 18 ns.

The fact that the E399Q mutation results in a loss of interactions to the maltopentaose raises the question as to whether this mutation lowers the propensity for maltopentaose to bind to the central binding region, leading to binding at the secondary site within the N-terminal region, as observed in 3VU2. Such secondary or surface binding sites have been reported to play important functional roles in other sugar binding enzymes, such as the targeting of substrate, facilitating the movement of the substrate into the active site, and controlling substrate specificity.[26] The maltopentaose binding site identified in 3VU2 could play any one of these roles. Alternatively as discussed by Wu et al.,[13] the function of SBE may require two chains to be bound simultaneously, the remnant chain with a minimum DP and the cleaved chain to be transferred. It is possible that the alternate binding site found in 3VU2 is the location where the chain that is to be transferred resides; however, the time scale of such a transition would be much longer than that currently accessible in atomistic simulations.

The Effect of Other Single-Point Mutations. Three single point mutations, E399D, R342K, and Y235F, were introduced into the apo 3AML crystal structure, and the resultant structure docked with maltopentaose. These mutations had been introduced by Li et al.[14] into corn SBEIIa, and their effect on the activity of the enzyme and the CLDs was

DOI: 10.1021/acs.biomac.5b00710
Biomacromolecules 2015, 16, 2475−2481

studied experimentally. Representative structures from the simulations of the different maltopentaose complexes are shown in Figure 6. Figure 6I shows key residues from the native enzyme (3AML) together with maltopentaose. As noted above, Glu399, His467, and Trp309 all formed stable interactions with maltopentaose, while Tyr235 and Arg342 interact with these residues. The equivalent structures from the simulations involving the three mutations are also shown: E399D (Figure 6II), R342K (Figure 6III), and Y235F (Figure 6IV). In the case of the mutation E399D, maltopentaose did not remain bound to the central cleft, but left the binding site within 2 ns in both simulations. In the native protein, the carboxyl group of Glu399 forms a stable interaction with the sugar. In the E399D mutant, Asp399 instead forms a stable salt bridge with the side chain of Arg342. This is consistent with the loss of activity by this mutant observed by Li et al.[14]

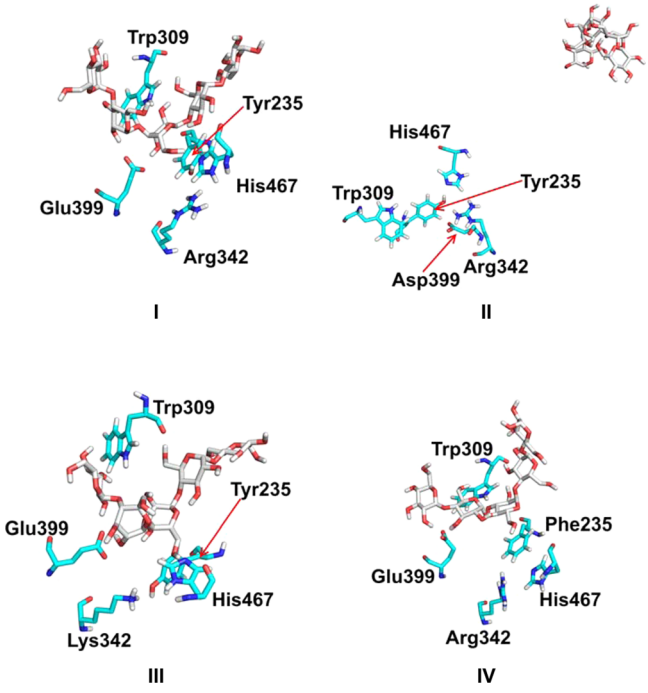

Figure 6. Three single point mutations introduced to 3AML. (I) The native enzyme with maltopentaose bound to the central cleft; Trp309, Glu399, Arg342, His467, and Tyr235 have been outlined. (II) The E399D mutation where glutamate was mutated to aspartic acid, (III) the R342 K mutation where arginine was mutated to lysine, and (IV) the Y235F mutation where tyrosine was mutated to phenylalanine.

R342K is the only mutation introduced by Li et al.[14] that resulted in a significant change in the CLD: specifically, this resulted in an increase in the proportion of shorter branches. The maltopentaose:SBEI R342 K complex was found to be stable over the 25 ns simulated. A representative structure is shown in Figure 6III. In the native SBE, Figure 6I, the Arg342 side chain interacts directly with His467, Glu399, and Tyr235. In the R342 K mutant, there is not only a decrease in the interactions with His467, Glu399, and Tyr235, but Tyr235 no longer interacts directly with His467. The change in CLD observed by Li et al. may result from an increase in mobility of Glu399 leading to the chain being cleaved in a more random manner, and hence more short branches.

Experimentally,[14] in SBEIIa the Y235F mutation was found to result in a total loss of activity. In the simulations of maltopentaose:3AML, the Y235F complex was found to be stable on a 25 ns time scale. However, critical interactions with the catalytically important His467 were lost. In the native form the side-chain hydroxyl of Tyr235 forms a stable interaction with the side chain of His467, with or without maltopentaose bound in the central cleft. This interaction is no longer possible in the case of Phe235. This leads to reorientation of the side chain of His467, providing an explanation of the observed loss of enzymatic activity.

Experimentally, E399D and Y235F resulted in a total loss of activity. In contrast, R342K altered the CLD resulting in shorter branches. As noted above, this could be explained by an increase in the mobility of Glu399, enabling it to interact with alternative sugars along the chain. This would suggest that restricting the movement and flexibility of Glu399 may lead to longer branches, potentially resulting in slower digesting starch.

CONCLUSIONS

Efforts to engineer SBEs in order to modulate the structure and hence the functional properties of starches have been met with limited success. One reason for this is a lack of a basic understanding of how SBEs and their substrates interact. In this work we have shown that a combination of molecular dynamics simulations and docking approaches can be used to identify key residues that could be targeted in future mutagenesis studies, and in this way help answer basic mechanistic questions important for the production of starch with improved functional properties. We have shown that the interaction of maltopentaose with the N-terminal region of SBE, as observed crystallographically in the case of the E399Q mutant, did not affect the geometry of the central binding region. We also showed that a number of residues proposed to be important for binding at this site (based on the available crystal structure) probably do not interact strongly with the sugar in free solution. By examining the binding of a range of different sized starch fragments to the central binding region, it was found that Trp309, Glu399 and His467 may play key roles in substrate recognition and that in *Oryza sativa L.* the minimal functional fragment size, X_{min}, is most likely 5. The work has also allowed us to examine the effects of three different point mutations on the interaction of rice SBE with maltopentaose and correlate this with experiment. The agreement of the simulations with a range of different types of data supports the validity of the approach.

In no case did the simulations indicate that these starch polymers form helical structures to the extent to that observed in the simulations in the presence of enzyme. This suggests that SBE may act as a template catalyzing the formation of the crystalline lamellae that are an essential feature of native starch. Of course all of the conclusions above depend to some degree on the accuracy of the initial model. In this study a combination of two different crystal structures was used. The study also relies heavily on docked complexes, which also inevitably introduces a degree of uncertainty. This said, the results obtained reproduce a range of experimental results suggesting the models are predictive. Furthermore, we have demonstrated that different docked structures converge to similar conformations, providing additional confidence in the validity of the results.

Overall, the work demonstrates the utility of such computation approaches in understanding these central biosynthetic systems at an atomic level and will hopefully

DOI: 10.1021/acs.biomac.5b00710
Biomacromolecules 2015, 16, 2475−2481

facilitate the development of "designer starches" with optimized functional properties.

■ ASSOCIATED CONTENT

Supporting Information

Computational details; electron density maps; RMS positional deviation values; distance between Glu45-maltopentaose (and Glu320(OE2)-maltopentaose as a function of time; distribution of RMSD values between pairs of structures; orientation of the different sized starch fragments in the central binding cleft; representative structures of different sized starch fragments; structures after 10 ns of simulation of various starch oligomers. The Supporting Information is available free of charge on the ACS Publications website at DOI: 10.1021/acs.biomac.5b00710.

■ AUTHOR INFORMATION

Corresponding Authors

*Fax: + 61 7 3365 4273; Telephone: +61 7 3365 7562; E-mail address: a.malde@uq.edu.au.

*Fax: +61 7 3365 1188; Telephone +61 7 3365 4809; E-mail address: b.gilbert@uq.edu.au.

Notes

The authors declare no competing financial interest.

■ ACKNOWLEDGMENTS

This work was supported but the Australian Research Council (ARC projects DP110100327 and DP150101097, with the assistance of high-performance computing resources provided by the National Computational Infrastructure National Facility and iVEC located at iVEC@Murdoch through the National Computational Merit Allocation Scheme (project m72) and ARC LE120100181. We gratefully acknowledge the support of the 1000-Talents Program of the Chinese Foreign Experts Bureau.

■ REFERENCES

(1) Wolever, T. M. S. *Nutr. Rev.* **2003**, *61*, S40−S48.

(2) Zhang, G.; Ao, Z.; Hamaker, B. R. *J. Agric. Food Chem.* **2008**, *56*, 4686−4694.

(3) Witt, T.; Gidley, M. J.; Gilbert, R. G. *J. Agric. Food Chem.* **2010**, *58*, 8444−8452.

(4) Satoh, H.; Nishi, A.; Yamashita, K.; Takemoto, Y.; Tanaka, Y.; Hosaka, Y.; Sakurai, A.; Fujita, N.; Nakamura, Y. *Plant Physiol.* **2003**, *133*, 1111−1121.

(5) Zeeman, S. C.; Kossmann, J.; Smith, A. M. *Annu. Rev. Plant Biol.* **2010**, *61*, 209−234.

(6) Yao, Y.; Thompson, D. B.; Guiltinan, M. J. *Plant Physiol.* **2004**, *136*, 3515−3523.

(7) Guan, H. P.; Preiss, J. *Plant Physiology* **1993**, *102*, 1269−1273.

(8) *The PyMOL Molecular Graphics System*, version 1.6; Schrödinger, LLC: New York, 2009−2013.

(9) Chaen, K.; Noguchi, J.; Omori, T.; Kakuta, Y.; Kimura, M. *Biochem. Biophys. Res. Commun.* **2012**, *424*, 508−511.

(10) Vu, N. T.; Shimada, H.; Kakuta, Y.; Nakashima, T.; Ida, H.; Omori, T.; Nishi, A.; Satoh, H.; Kimura, M. *Biosci., Biotechnol., Biochem.* **2008**, *72*, 2858−2866.

(11) van der Maarel, M. J. E. C.; van der Veen, B.; Uitdehaag, J. C. M.; Leemhuis, H.; Dijkhuizen, L. *J. Biotechnol.* **2002**, *94*, 137−155.

(12) Nakamura, A.; Haga, K.; Yamane, K. *Biochemistry* **1993**, *32*, 6624−6631.

(13) Wu, A. C.; Gilbert, R. G. *Biomacromolecules* **2010**, *11*, 3539−3547.

(14) Li, C.; Wu, A. C.; Go, R. M.; Malouf, J.; Turner, M. S.; Malde, A. K.; Mark, A. E.; Gilbert, R. G. *PLoS One* **2015**, *10*, e0125507.

(15) Nielsen, T. H.; Baunsgaard, L.; Blennow, A. *J. Biol. Chem.* **2002**, *277*, 20249−20255.

(16) Noguchi, J.; Chaen, K.; Vu, N. T.; Akasaka, T.; Shimada, H.; Nakashima, T.; Nishi, A.; Satoh, H.; Omori, T.; Kakuta, Y.; Kimura, M. *Glycobiology* **2011**, *21*, 1108−1116.

(17) van der Spoel, D.; Lindahl, E.; Hess, B.; Groenhof, G.; Mark, A. E.; Berendsen, H. J. C. *J. Comput. Chem.* **2005**, *26*, 1701−1718.

(18) Schmid, N.; Eichenberger, A. P.; Choutko, A.; Riniker, S.; Winger, M.; Mark, A. E.; van Gunsteren, W. F. *Eur. Biophys. J.* **2011**, *40*, 843−856.

(19) Lins, R. D.; Hünenberger, P. H. *J. Comput. Chem.* **2005**, *26*, 1400−1412.

(20) Malde, A. K.; Zuo, L.; Breeze, M.; Stroet, M.; Poger, D.; Nair, P. C.; Oostenbrink, C.; Mark, A. E. *J. Chem. Theory Comput.* **2011**, *7*, 4026−4037.

(21) Guex, N.; Peitsch, M. C. *Electrophoresis* **1997**, *18*, 2714−2723.

(22) Daura, X.; Gademann, K.; Jaun, B.; Seebach, D.; van Gunsteren, W. F.; Mark, A. E. *Angew. Chem., Int. Ed.* **1999**, *38*, 236−240.

(23) Matsui, I.; Yoneda, S.; Ishikawa, K.; Miyairi, S.; Fukui, S.; Umeyama, H.; Honda, K. *Biochemistry* **1994**, *33*, 451−458.

(24) Gilbert, R. G. *Anal. Bioanal. Chem.* **2011**, *399*, 1425−1438.

(25) Seviour, T.; Malde, A. K.; Kjelleberg, S.; Yuan, Z.; Mark, A. E. *Biomacromolecules* **2012**, *13*, 1965−1972.

(26) Cockburn, D.; Wilkens, C.; Ruzanski, C.; Andersen, S.; Willum Nielsen, J.; Smith, A. M.; Field, R. A.; Willemoës, M.; Abou Hachem, M.; Svensson, B. *Biologia* **2014**, *69*, 705−712.

DOI: 10.1021/acs.biomac.5b00710
Biomacromolecules 2015, 16, 2475−2481